研究報告書

①氏名、所属機関および学年：
小野寺陽平（京都大学工学研究科機械理工学専攻　博士後期課程 3 年）

②課題番号、利用ビームライン、および課題名：
2009A1644、BL-04B2、
「超イオン伝導体 Li2S-P2S5 非平衡結晶の構造研究」
Structural study of superionic conductor Li2S-P2S5 meta-stable crystal

③研究概要：

1. Background

A $(Li_2S)_x(P_2S_5)_{100-x}$ glass, which can be synthesized by mechanical alloying, is an excellent lithium ionic conductor, showed a high ionic conductivity in the order of 10^{-4} S/cm at room temperature (RT).[1] In addition, around x = 70, $Li_7P_3S_{11}$ non-equibrium crystal (as known glass ceramics) can be obtained by aging the $(Li_2S)_{70}(P_2S_5)_{30}$ glass at 513 K, and its ionic conductivity drastically increases up to more than 10^{-3} S/cm.[2] Therefore, the $Li_7P_3S_{11}$ has attracted much attention as a solid electrolyte of rechargeable lithium ion batteries.

In recent synchrotron X-ray powder diffraction (SXPD) experiments, the crystal structure of $Li_7P_3S_{11}$ was refined on the basis of the $P\bar{1}$ symmetry in the triclinic system.[3] It was found that PS_4 tetrahedra and P_2S_7 ditetrahedra are contained in $Li_7P_3S_{11}$ and Li ions are situated between them. However, it seems that the atomic coordinates of Li, determined by SXPD, are still controversial, because in the case of X-ray scattering the atomic scattering factor, $f(\sin\theta/\lambda)$, of Li is much small. On the other hand, neutron powder diffraction (NPD) is a powerful technique to determine precisely the atomic coordinates of light elements such as hydrogen and lithium, because they have large enough neutron scattering cross sections comparable to those of other elements, if we use isotopes of hydrogen and lithium (D and ^{7}Li). Therefore, the NPD surely gives us precise atomic coordinates of Li and valuable hints to understand the mechanism of the fast lithium ionic conduction on $Li_7P_3S_{11}$.

In this work, a ^{7}Li isotope enriched $^7Li_7P_3S_{11}$ glass ceramics was prepared for the NPD and the SXPD experiments. It is noteworthy that the use of ^{7}Li is to reduce background intensities on a NPD pattern. We determine the detailed crystal structure of $Li_7P_3S_{11}$ by the combined X-ray/neutron Rietveld analysis.

2. Experimental procedure

$^7Li_7P_3S_{11}$ glass ceramics was synthesized by the heat treatment of the $(^7Li_2S)_{70}(P_2S_5)_{30}$ glass, which was prepared by the mechanical alloying of the mixture of $^7Li_2S$ (Koujundo Chem., 99.9%, isotropic enrichment of ^{7}Li ≦99.94%), P (Mitsuwa Chem., 99.999%), and S (Koujundo Chem., 99.99%) powders with a planetary ball mill apparatus (Fritsch, P-5), a zirconia pot (a volume of 80 cc), and 20 zirconia balls (10 mmϕ). The detailed mechanical alloying and heat treatment processes were as follows. In the nominal molar proportion of P_2S_5, the P and the S powders were mechanically mixed at 300 rpm for 150 h under the high purity argon gas atmosphere, and then $^7Li_2S$ powder was added to the mixture and mechanically milled again at 300 rpm for 50 h. The obtained $(^7Li_2S)_{70}(P_2S_5)_{30}$ glass was put into a vacuum-packed borosilicate glass tube, and heated at 523 K for 2 h, followed by quick cooling to RT.

The SXPD experiments were carried out on the horizontal two-axis diffractometer (E = 61.60 keV, λ = 0.02013 nm) at the BL04B2 beam line of the SPring-8 synchrotron radiation facility.[4] The $^7Li_7P_3S_{11}$ glass ceramics was put into a stainless seal cell with capton windows in argon gas, and a SXPD pattern was collected at RT for 2 h. We also measured a time-of-flight NPD (TOF-NPD) pattern at RT for 5 h on the General Material Diffractometer (GEM),[5,6] installed at the ISIS in the UK Rutherford Appleton Laboratory. The $^7Li_7P_3S_{11}$ was put into a cylindrical vanadium can of 8 mm diameter in argon gas. Later, the crystal structure of $^7Li_7P_3S_{11}$ was refined by using the Rietveld analysis program, GSAS, with

the EXPGUI interface.[7-9)]

3. Results and discussion

The TOF-NPD and SXPD patterns at RT are shown in Figs. 1(a) and (b), respectively. The combined X-ray/neutron Rietveld analysis was carried out with the same crystal structure model of the $P\bar{1}$ symmetry, as mentioned in Introduction.[3)] For all sites of Li, P, and S their occupancies, *g*, were fixed to be 1.0 (no deficiency). Consequently, we obtained a good fit between observed and calculated patterns: χ^2 = 30.74 and R_{wp} = 5.68%, and confirmed that no superlattice reflections appear on both of TOF-NPD and SXPD patterns. The lattice parameters were estimated as a =12.483(2) Å, b = 6.0310 (5) Å, c = 12.499(1) Å, α = 102.906(11) °, β = 113.304(8) °, and γ = 74.495(11) °. The detailed structure parameters, atomic coordinates (x, y, z) and an equivalent isotropic atomic displacement parameter (U_{iso}), are listed in Table I.

The refined crystal structure of $^7Li_7P_3S_{11}$ is shown in Fig. 2. A $[P_2S_7]^{4-}$ ditetrahedron and a $[PS_4]^{3-}$ tetrahedron consist of {(S1/S2/S3/P1)–S4–(P2/S5/S6/S7)} and (P3/S8/S9/S10/S11), surrounded by Li^+ cations. Note that the charge valences of Li, P, and S are 1+, 5+, and 2–, according to charge neutrality. All bond lengths between P and S, $l_{P\text{-}S}$, in P_2S_7 and PS_4 are listed in Table II; each PS_4 is obviously a slightly distorted tetrahedron. Furthermore, we focused on the bond lengths between Li and S, $l_{Li\text{-}S}$, around P_2S_7 and PS_4, summarized at the r-region between 2.2 and 2.8 Å, as shown in Fig. 3 and Table III. As a result, the distribution of $l_{Li\text{-}S}$ around PS_4 was narrower than that around P_2S_7. This distribution of $l_{Li\text{-}S}$ is also in good agreement with the reduced pair distribution function, *G(r)*, obtained by the Fourier transformation of total scattering factor *S(Q)*, which will be reported elsewhere. To clarify the mechanism of the fast lithium ionic conduction in $Li_7P_3S_{11}$ it is important to predict the diffusion pathway of Li^+ cations, and even more important to visualize a network of neighboring Li^+ cations. Figure 4 schematically illustrates Li–Li correlations (solid gray lines) within 3.7 Å. Interestingly, it was found that the Li–Li chains zigzag through open space between P_2S_7 ditetrahedra and PS_4 tetrahedra, as indicated by the black circle in Fig. 4. In contrast, the Li–Li chains do not appear on the open space between two P_2S_7 ditetrahedra (solid gray circle). Presumably, this result suggests that a favorite diffusion pathway with Li^+ cations is close to the Li–Li chains. Even though we are still unsure where a lot of interstitial sites of Li are, the visualized network of neighboring Li^+ cations would be beneficial to comprehend the mechanism of the fast lithium ionic conduction on $Li_7P_3S_{11}$ in our future work.

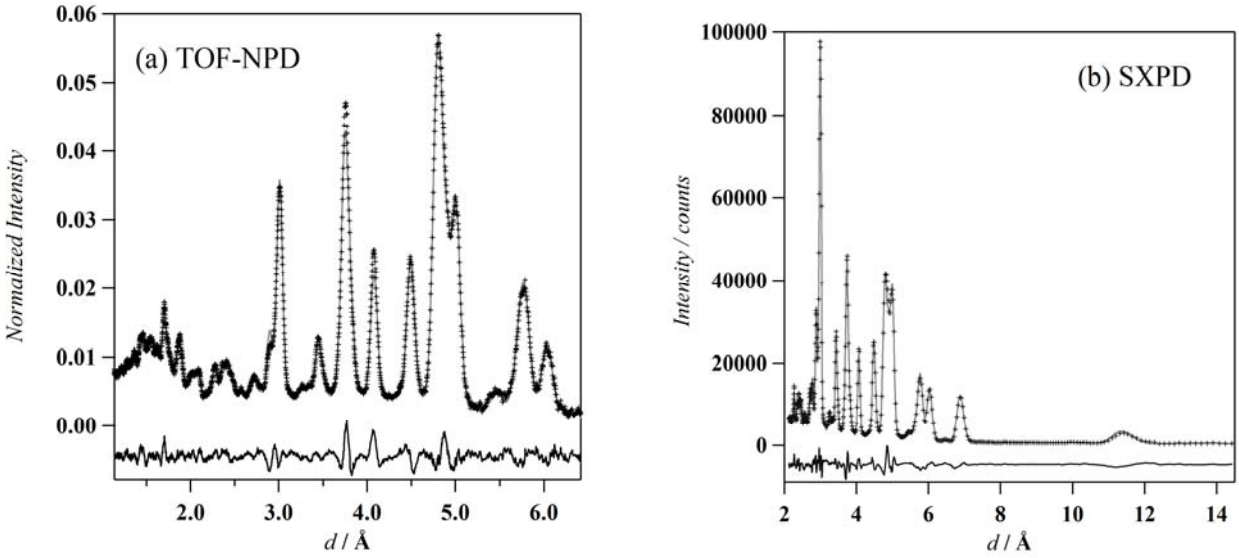

Fig. 1. Rietveld refinement patterns of $^{7}Li_7P_3S_{11}$ glass ceramics: time-of-flight neutron powder diffraction (TOF-NPD) (a), and synchrotron X-ray powder diffraction (SXPD) (b), respectively. Plus marks are observed intensities, and solid gray lines are calculated ones. Curves at the bottom are the difference between the observed and the calculated patterns.

Table I. Structure parameters of $^{7}Li_7P_3S_{11}$ glass ceramics at RT.

Atom	**x**	**y**	**z**	U_{iso} **(Å^2)**
^{7}Li1	0.6764(7)	0.1305(16)	0.1449(7)	0.75(10)
^{7}Li2	0.6182(6)	0.6225(9)	0.8685(4)	0.43(5)
^{7}Li3	0.2675(7)	0.4910(14)	0.7345(6)	0.69(8)
^{7}Li4	–0.0732(11)	0.8322(17)	0.2341(8)	0.80(9)
^{7}Li5	0.3147(6)	0.6493(15)	0.2815(5)	0.80(8)
^{7}Li6	0.6635(7)	0.7505(17)	0.5118(5)	0.06(3)
^{7}Li7	0.1223(6)	0.1007(16)	0.1285(6)	0.80(8)
P1	0.7918(4)	0.0549(15)	0.4733 (5)	0.158(9)
P2	0.4887(6)	0.0101(11)	0.3004(4)	0.11(1)
P3	0.8426(6)	0.2573(9)	0.0709(5)	0.18(1)
S1	0.8522(4)	0.2098(16)	0.6389(5)	0.27(1)
S2	0.8321(6)	0.1398(9)	0.3525(4)	0.092(8)
S3	0.8379(5)	–0.3052(15)	0.4645(5)	0.011(4)
S4	0.6093(4)	0.1714(8)	0.4440(4)	0.102(7)
S5	0.3232(3)	0.2098(7)	0.2830(4)	0.016(6)
S6	0.5235(5)	0.0124(10)	0.1580(6)	0.121(9)
S7	0.5133(3)	–0.3374(7)	0.3016(4)	0.054(7)
S8	0.8472(5)	0.3285(8)	–0.0767(4)	0.047(8)
S9	0.8272(5)	–0.0907(10)	0.0380(3)	0.092(9)
S10	0.6758(6)	0.4802(10)	0.0606(4)	0.008(4)
S11	0.9648(6)	0.3757(15)	0.2098(6)	0.003(3)

For all sits of Li, P, and S, g = 1.0, where g is the occupancy.

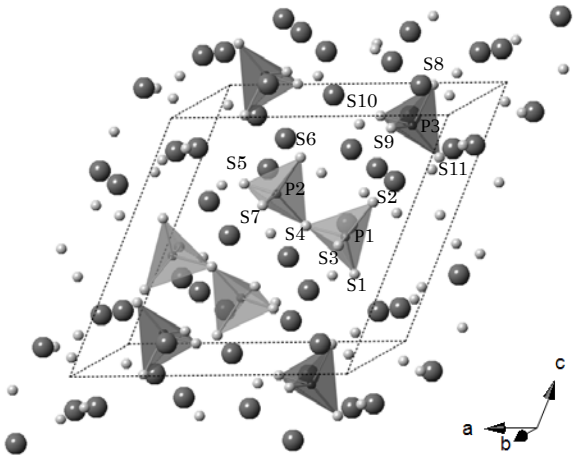

Fig. 2. Crystal structure of $^{7}Li_7P_3S_{11}$ glass ceramics at RT. Dark tetrahedra are PS_4, and bridging tetrahedra are P_2S_7, respectively. Black spheres are Li^+ cations. A broken line means the unit cell of crystal.

Table II. Bond lengths between P and S in P_2S_7 and PS_4 (Å).

$l_{P\text{-}S}$ in P_2S_7 [Å]				$l_{P\text{-}S}$ in PS_4 [Å]	
P1 – S1	2.000(5)	P2 – S4	2.074(4)	P3 – S8	2.011(5)
P1 – S2	1.970(5)	P2 – S5	2.048(4)	P3 – S9	2.093(5)
P1 – S3	2.082(5)	P2 – S6	1.996(4)	P3 – S10	2.128(5)
P1 – S4	2.101(5)	P2 – S7	2.037(4)	P3 – S11	1.945(5)

Table III. Important bond lengths between Li and S (Å).

Li1 - S2	2.553(5)	Li3 – S3	2.475(5)	Li5 – S8	2.563(4)
Li1 – S6	2.280(5)	Li3 – S10	2.349(4)	Li6 – S3	2.393(5)
Li1 – S9	2.641(4)	Li4 – S1	2.556(5)	Li6 – S4	2.686(5)
Li1– S10	2.555(5)	Li4 – S2	2.452(5)	Li6 – S5	2.464(4)
Li2 - S5	2.734(4)	Li4 – S9	2.360(4)	Li6 – S7	2.593(4)
Li2 – S6	2.419(5)	Li4 – S11	2.633(5)	Li7 – S5	2.640(5)
Li2 – S7	2.700(4)	Li5 – S1	2.523(5)	Li7 – S8	2.486(5)
Li2– S10	2.503(4)	Li5 – S5	2.627(4)	Li7 – S9	2.384(4)
Li3 – S2	2.498(5)	Li5 – S7	2.414(4)	Li7 – S11	2.595(4)

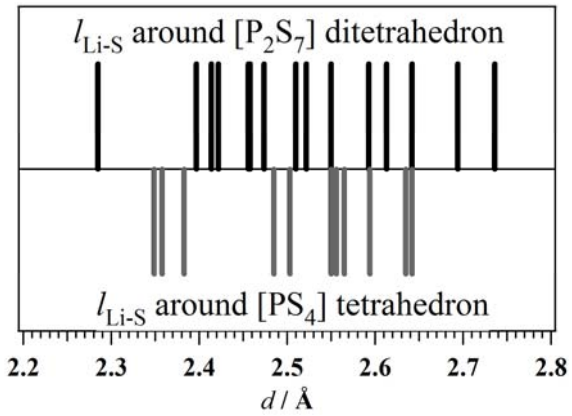

Fig. 3. Distribution of bond lengths between Li and S: vertical black lines correspond to $l_{Li\text{-}S}$ around P_2S_7, and gray ones $l_{Li\text{-}S}$ around PS_4, respectively.

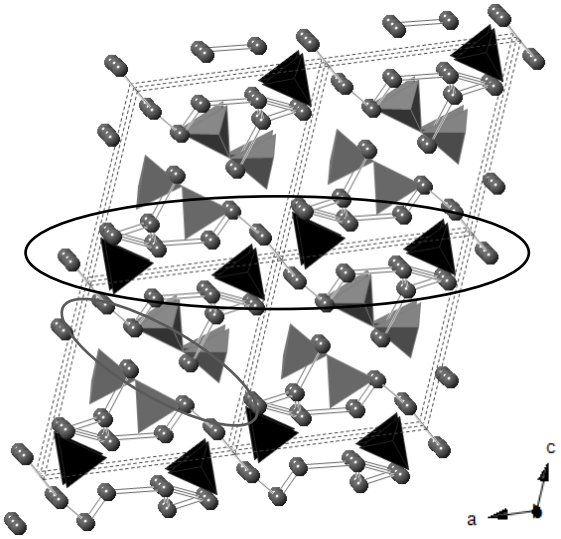

Fig. 4. Visualized network of neighboring Li^+ cations. Solid gray lines are Li–Li correlations within 3.7 Å. In the black circle Li–Li chains zigzag through open space between P_2S_7 ditetrahedra (gray) and PS_4 tetrahedra (black), whereas in the gray circle such a Li–Li chain is not observed. A broken line means the crystal of unit cell.

References

1) F. Mizuno, A. Hayashi, K. Tadanaga and M. Tatsumisago: Adv. Mate. **17** (2005) 134.
2) T. Ohtomo, F. Mizuno, A. Hayashi, K. Tadanaga and M. Tatsumisago: Solid State Ionics **176** (2005) 2349.
3) H. Yamane, M. Shibata, Y. Shimane, T. Junke, Y. Seino, S. Adams, K. Minami, A. Hayashi and M. Tasumisago: Solid State Ionics **178** (2007) 1163.
4) S. Kohara, K. Suzuya, Y. Kashihara, N. Matsumoto, N. Umesaki and I. Sakai: Nucl. Instrum. and Meth. A **467-468** (2001) 1030.
5) W.G. Williams, R.M. Ibberson, P. Day and J.E. Enderby: Physica B **241–243** (1998) 234.
6) A.C. Hannon: in: J. Lindon, G. Tranter, J. Holmes (Eds.), Encyclopedia of Spectroscopy and Spectrometry, vol. 2, Academic Press, London, 2000, p. 1479.
7) H. M. Rietveld: J. Appl. Crystallogr. **2** (1969) 65.
8) A. C. Larson, R. B. von-Dreele: Los Alamos National Laboratories, Report LAUR **86** (1994) 748.
9) B. H. Toby: J. Appl. Crystallogr. **34** (2001) 2